



This is a repository copy of *Pursuing safer batteries: Thermal abuse of LiFePO₄ cells.*

White Rose Research Online URL for this paper:
<http://eprints.whiterose.ac.uk/141067/>

Version: Accepted Version

Article:

Bugryniec, P., Davidson, J., Cumming, D. et al. (1 more author) (2019) Pursuing safer batteries: Thermal abuse of LiFePO₄ cells. *Journal of Power Sources*, 414. pp. 557-568. ISSN 0378-7753

<https://doi.org/10.1016/j.jpowsour.2019.01.013>

Article available under the terms of the CC-BY-NC-ND licence
(<https://creativecommons.org/licenses/by-nc-nd/4.0/>).

Reuse

This article is distributed under the terms of the Creative Commons Attribution-NonCommercial-NoDerivs (CC BY-NC-ND) licence. This licence only allows you to download this work and share it with others as long as you credit the authors, but you can't change the article in any way or use it commercially. More information and the full terms of the licence here: <https://creativecommons.org/licenses/>

Takedown

If you consider content in White Rose Research Online to be in breach of UK law, please notify us by emailing eprints@whiterose.ac.uk including the URL of the record and the reason for the withdrawal request.



eprints@whiterose.ac.uk
<https://eprints.whiterose.ac.uk/>

Pursuing safer batteries: thermal abuse of LiFePO₄ cells

Peter J. Bugryniec^a, Dr Jonathan N. Davidson^b, Dr Denis J. Cumming^a, Dr Solomon F. Brown^{a,*}

^aDepartment of Chemical & Biological Engineering, University of Sheffield, Sheffield, S1 3JD, England

^bDepartment of Electronic & Electrical Engineering, University of Sheffield, Sheffield, S1 4DE, England

Abstract

In this paper, accelerated rate calorimetry (ARC) and oven exposure, are used to investigate thermal runaway (TR) in lithium-ion cells. Previous work shows that lithium iron phosphate (LFP) cells have a lower risk of TR over other Li-ion chemistries. ARC is carried out on cells at various SOC to identify which decomposition reactions are contributing to the TR behaviour of a cell at different SOC. Results show, at SOC of 100% and 110%, the negative and positive electrode reactions are the main contributors to TR, while at lower SOC it is the negative electrode reaction that dominates. Cells at 100% SOC exposed to high temperatures during oven tests show, along with the ARC analysis, that the presence of the cathode and electrolyte reactions leads to an increase in the severity of a TR event for oven temperatures above 200°C. By comparing the heat generated in ARC and oven testing, it is shown that ARC does not fully capture the self-heating and TR safety hazard of a cell, unlike oven testing. This work gives new insight into the nature of the decomposition reactions and also provides an essential data set useful for model validation which is of importance to those studying LFP cells computationally.

Keywords: Thermal Runaway, Lithium Iron Phosphate Cells, Accelerated Rate Calorimetry, Oven Abuse Test, Li-ion

1. Introduction

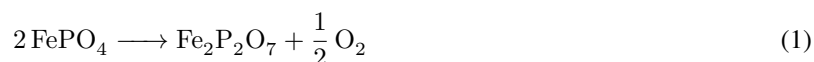
Lithium-ion (Li-ion) rechargeable batteries (LIBs) have become the most popular battery for portable electronics due to their high energy density, high cycle efficiency and low self-discharge (Kim et al., 2012; Placke et al., 2017). However, when abused, Li-ion cells can suffer from thermal runaway (TR) which can lead to fire and explosion of a cell (Wang et al., 2012; Lisbona and Snee, 2011; Ohsaki et al., 2005). Additionally, with the concern over global CO₂ emissions, the use of LIBs as energy storage devices is increasing due to development of hybrid and fully-electric vehicles, and the development of energy storage systems for stationary applications to aid in the utilisation of renewable energy generation (International Energy Agency, 2016; IRENA and IEA-ETSAP, 2012; Palizban and

*Corresponding author

Email address: s.f.brown@sheffield.ac.uk (Dr Solomon F. Brown)

[Kauhaniemi, 2016](#); [Leadbetter and Swan, 2012](#)). TR poses a significant problem for emerging applications that have ever-greater energy density demands ([Doughty and Roth, 2012](#)). Increased capacity leads to an increased safety risk because a critical failure of a high-capacity LIB will be more energetic and therefore pose a greater hazard. Hence there is a need to reduce the probability and severity of TR, and to understand the mechanisms behind TR.

Previous work in the literature has shown that lithium iron phosphate (LFP), LiFePO_4 , cells are the safest of the many types of Li-ion cell chemistries (LiCoO_2 , LiMn_2O_4 , LiNiMnCoO_2 , LiNiCoAlO_2 , LiNiO_2 , LiNiCoO_2 , LiNiCoTiMgO_2) available, with increased thermal stability and reduced hazard of TR ([Chen and Richardson, 2010](#); [Golubkov et al., 2014](#); [Jiang and Dahn, 2004b](#); [Liu et al., 2016](#); [Lu et al., 2013](#); [MacNeil et al., 2002](#); [Lei et al., 2017](#)). LFP cells' increased stability is believed to be due to the inhibition of oxygen loss by strong covalent P-O bonds in the cathode ([Chen and Richardson, 2010](#)). For LFP cells, the cathode decomposes releasing oxygen according to [Equation 1](#) ([Khakani et al., 2016](#)). The lack of available oxygen limits the amount of electrolyte that can be ignited during TR, vastly reducing the amount of heat produced and in turn reducing the overall severity of TR. For example, the calculated release of oxygen for an 18650 LFP cell is 0.5 g compared to 3.25 g for a comparable lithium cobalt oxide (LCO) cell ([Chen et al., 2015](#)). The amount of oxygen available is also influenced by the cells' SOC, specifically the lithiation state of the cathode. The amount of oxygen available is greater for charged cells (cathode delithiated), while even at 0% SOC there may still be small amounts of O_2 released, as the cathode can not be fully lithiated due to irreversible capacity loss during the formation cycles of the cell ([Golubkov et al., 2015](#)).



Despite the significant safety advantages of LFP cells over that of other Li-ion chemistries, there exists a lack of knowledge describing the exothermic reactions during TR of LFP cells. For other chemistries, TR has been widely assessed by several abusive methods from which cell safety can be quantified. These include overheating, penetration, crush, overcharge and short circuiting ([Spotnitz and Franklin, 2003](#); [Feng et al., 2018](#)). Overheating or thermal abuse tests are key to providing data on the stability and severity of TR, and as such, are the focus of this paper. This category of testing can be carried out in several ways, including by accelerated rate calorimetry (ARC) and convection oven tests. However, LFP cells have not been comprehensively assessed over various states of charge (SOC) under ARC with the aim to determine the sequence of reactions at each SOC. This criteria would allow understanding of the exothermic reactions taking place, and, in turn, a risk to be associated as a function of SOC. Beside preliminary studies in our previous work ([Bugrynec et al., 2018](#)) to determine the TR risk of LFP cells due to rapid external heating, the TR characteristics of LFP cells under convection oven tests have not been investigated.

The exothermic reactions taking place during TR of a Li-ion cell are commonly listed as, but not necessarily lim-

Table 1: Heat released by negative (carbon) and positive (LFP) electrode reactions

Reaction	Heat released, ΔH ($J g^{-1}$)	Reference
NE*	~1300 - 2800	(Roth and Doughty, 2004; Belharouak et al., 2007; Kvasha et al., 2018)
PE	~150 - 340	(Yamada et al., 2001; Takahashi et al., 2002; Chen and Richardson, 2010; Kvasha et al., 2018)

* Heat released in negative reaction includes SEI reaction.

ited to: (1) solid electrolyte interphase (SEI) reaction; (2) negative-solvent (NE) reaction; (3) positive-solvent (PE) reaction; (4) electrolyte decomposition (Richard and Dahn, 1999a,b; Spotnitz and Franklin, 2003; Melcher et al., 2016). Identifying when these separate reactions occur and the energy they release allows one to attribute the contributions of individual reactions to the TR behaviour of a whole cell. The literature has shown that the SEI reaction begins to release heat at 50–120°C with maximum heat release at 253–300°C (Roth and Doughty, 2004; Abraham et al., 2006). A carbon/graphite anode has a heat release onset temperature between 80–160°C and exhibits peak self-heating between 200–350°C (Richard and Dahn, 1999b; MacNeil et al., 2000; Roth and Doughty, 2004; Belharouak et al., 2007; Ben Mayza et al., 2011). LFP cathodes at 100% SOC have a heat release onset temperature between 180–250°C and exhibit peak heating between 210–360°C (Yamada et al., 2001; MacNeil et al., 2002; Takahashi et al., 2002; Jiang and Dahn, 2004b,a). Takahashi et al. (2002) also show that the fully discharged LFP cathode presents no self-heating up to 400°C. ARC test on LFP cathodes in electrolyte show two exotherms (Khakani et al., 2016). The first is thought to be due to the decomposition of the salt ($LiPF_6$) additive in the electrolyte decomposing on the surface of the electrode, before the second reaction that is the decomposition of the LFP cathode its self. Table 1 lists the heat released by the NE (which include the SEI reaction) and PE reactions. For LFP cells it can be clearly seen that the NE reaction is the major contributor to the TR potential of the cell. At high temperatures (>250°C), the electrolyte can ignite in the presence of oxygen releasing large amounts of heat (Chen and Richardson, 2010). Hence, for the solvent reaction to occur, decomposition of the LFP cathode is required (assuming that the cell is intact such that no oxygen can enter from the environment into the cell) (Khakani et al., 2016). The most significant reactions during TR are the strongly exothermic combustion of carbonous material and Li oxidation, which are affected by the amount of available O_2 and intercalated Li in the anode (both greater at increased SOC), respectively (Golubkov et al., 2015). This data can be used to infer the process of TR in cells abused by ARC and oven tests.

Li-ion cells have been studied by adiabatic calorimetry methods, including ARC (Jiang and Dahn, 2004b; Ben Mayza et al., 2011; Ishikawa et al., 2012; Mendoza-Hernandez et al., 2015; Lei et al., 2017), vent sizing package 2 (VSP2) (Jhu et al., 2012; Wen et al., 2012; Chen et al., 2015) and copper slug (constant power) calorimetry (Liu et al., 2016). Adiabatic calorimetry is used to determine the stability (i.e. onset temperature of TR) and severity of TR. The temperature rate is of most interest as it is directly proportional to the heat generation rate and, in turn, is an indicator

of the cooling required to keep self-heating under control and prevent TR.

Previous calorimetry experiments have quantified the severity of TR in LFP cells at 100% SOC (Lei et al., 2017; Jhu et al., 2012; Wen et al., 2012; Ben Mayza et al., 2011). The study of Li-ion cells of other chemistries at various SOC have shown that cells at a lower SOC are more stable and safer than their fully charged counterparts, and studies of this type also allows a safe operating window for a cell in terms of SOC and temperature to be determined (Jhu et al., 2011; Ishikawa et al., 2012; Mendoza-Hernandez et al., 2015; Liu et al., 2016). Some studies have investigated TR at various SOC in LFP cells (Lu et al., 2013; Kvasha et al., 2018; Perea et al., 2018), and show similar characteristic behaviour to other chemistries. However, they do not discuss the nature of the reactions taking place at each SOC or define a safe operational window of the cells. Further, studying cells at SOC greater than 100% is important, as cells which are in an overcharged state not only present a more severe TR event due to the increased energy stored, but also a reduction in stability due to Li-plating on the anode (Mendoza-Hernandez et al., 2015; Golubkov et al., 2015; Li et al., 2014; Waldmann et al., 2018).

For LFP cells under calorimetry testing, Lu et al. (2013) showed that the only significant change at a lower SOC (open circuit voltage of 3.3 V compared to 3.65 V) was the temperature rate reducing by 75%. The increase in onset temperature (which represents increased stability) at lower SOC of Li-ion cells is due to the influence of lithiation on the thermal stability of the electroactive materials within a cell (Mendoza-Hernandez et al., 2015). Further, Kvasha et al. (2018) show that for LFP 18650 cells at 0%, 50% and 100% SOC, there is a reduced temperature rate with lower SOC, from $4.4^{\circ}\text{C min}^{-1}$ to $1.8^{\circ}\text{C min}^{-1}$. Additionally, with lower SOC there is an increased time to occurrence of exothermic reactions (Perea et al., 2018). However, Kvasha et al. (2018) also shows, from separate differential scanning calorimetry (DSC) results, that the peak heat release for the electrolyte, anode and cathode decomposition reactions occurs between 280°C and 300°C at all SOC. Thus the sequence of reactions can not be predicted from DSC, as it does not correlate with the peak rates, and hence heat released, in ARC test. As such, experiments on complete cells are required for a full understanding of the TR behaviour (Golubkov et al., 2015). The amount of heat released from an LFP cathode is shown to be less sensitive to SOC than the carbon anode, whereby, the heat released from the anode increases by an order of magnitude between 0% and 100% (Kvasha et al., 2018). Further, in the case of LFP cells, it has been shown that a lithiated (graphite) anode is more reactive than a delithiated (LFP) cathode (Ben Mayza et al., 2011; Wen et al., 2012; Kvasha et al., 2018); i.e, in a fully charged LFP cell the anode may provide more heat during TR than the LFP cathode. Ishikawa et al. (2012) and Mendoza-Hernandez et al. (2015) show that, from studying metal oxide cathodes, thermal maps are useful to determine if self-heating is self-sustaining and hence a safety issue.

Oven tests on Li-metal-oxide cells under constant oven temperatures (Hatchard et al., 2001; Jiang et al., 2004)

and under thermal ramping to a desired oven temperature (Tobishima and Yamaki, 1999) show that ovens at higher temperatures cause TR more quickly and result in higher cell temperatures during TR. Tobishima and Yamaki (1999) also shows that a relatively small increase in oven temperature can mean the difference between no TR and a severe TR event. Golubkov et al. (2014) shows that discharged LFP cells, under adiabatic-like constant power heating, did not go into TR below 250°C. For cells at 100% SOC, TR did occur and the maximum cell temperatures reached were between 400°C and 450°C. Further work by Golubkov et al. (2015), under similar conditions, compares NCA and LFP 18650 cells at various SOC, including overcharge. They show that the cells under TR produce high amounts of flammable gases, specifically CO, H₂ and CO₂. LFP cells produced less CO and H₂ than NCA, while both cells produced mainly CO₂ when discharged, and increasing amounts of CO and H₂ at higher SOC. Larsson and Mellander (2014) also studied LFP cells; however, this was for pouch cells under forced convection. Lei et al. (2017) shows that oven exposure leads to higher reaction rates at lower temperatures for a given cell compared to ARC. Hatchard et al. (2001) and Lopez et al. (2015) show the importance of oven abuse experiments in validating computational simulations of LiCoO₂ undergoing TR. However, a lack of oven test data for LFP 18650 cells presents an obstacle in validating similar computational work on LFP cells (see, for example the work by Peng and Jiang (2016)), and hence shows the necessity and a practical application of this work.

In this paper we will characterise the safety of LFP cells under thermal abuse conditions (ARC and convection oven tests) to quantify their safe operating window in terms of SOC and temperature, and identify the hazards they pose. Calorimetry is carried out under near-adiabatic conditions and represents the worst case scenario of a cell under heating, as there is zero heat loss from the cell. ARC also allows us to infer the process by which TR occurs, which is necessary for developing accurate models of TR by ensuring that the reactions are simulated in the correct order and with the appropriate magnitude of heat relative to each other (Ben Mayza et al., 2011). A convection oven test allows us to study the response of a cell when rapidly exposed to high temperatures, representing what might occur due environmental conditions or as a result of heating from a neighbouring cell which has failed by other means.

The aim of this work is to address gaps in the literature with regard to the TR behaviour of LFP cells under thermal abuse. The objectives of this work are: (1) to carry out a comprehensive analysis of 18650 LFP cells under ARC at various SOC to allow for a detailed understanding of the self-heating characteristics as a function of SOC and temperature; (2) to carry out convective heating oven abuse tests to analyse the thermal response under rapid heating, providing essential data for LFP TR model validation; (3) quantify the severity of TR, present a detailed description of the TR process and discuss how TR can be avoided in LFP cells using the results from objectives (1) and (2); (4) determine the energy released in each abuse test/ scenario for a comparison of test suitability in determining cell safety and TR characterisation.



Figure 1: Experimental set up of abuse tests (a) Thermal Hazard Technology ARC EV+ (b) close up of cell in ARC with thermocouple attached (TC) and suspended from aluminium frame in ARC vessel (c) convection oven (d) close up of cell in oven with TC placements.

2. Methodology

Experimental studies were carried out on commercial 1500 mAh LiFePO_4 , cylindrical 18650, cells (hereafter referred to as the LFP cell). The precise cell chemistry is currently unknown and unavailable from the manufacturer. Two experimental methods were used to characterise the TR behaviour of the LFP cells. The first method was an ARC test, while the second was abuse by overheating in an oven test. The set up of each experiment is shown in [Figure 1](#). The ARC test was carried out with cells at 0%, 28%, 63%, 100% and 110% SOC, while the oven test was carried out with cells at 100% SOC.

These LFP cells were charged to their required state of charge using the constant current - constant voltage (CC -

CV) method on a *MACCOR 4000M* battery cycler. Prior to charging, as cells were stored partially charged, all cells were discharged at 0.5C until 2.5 V, then at CV until the current dropped below 0.01C. To charge, a CC of 0.5C (0.75 A) was applied until the charge voltage is reached e.g. 3.65 V for 100% SOC, thereafter a CV (of e.g. 3.65 V) was applied until the charge current dropped below 0.01C. For a SOC of 28% and 63%, the cells were charged at 0.5C, with a CC cut off criterion determined by the corresponding charge capacity for the desired SOC (420 mAh and 945 mAh respectively). For 0% SOC, the cell was discharged but not recharged. For overcharge at 110%, the cell is charged at 0.5C until 4.2 V, then at 0.2C to reduce ohmic heating, cut off is determined by capacity (1650 mAh).

2.1. ARC Test

The ARC tests were performed using a *Thermal Hazard Technology ARC EV+* calorimeter, see [Figure 1\(a\)](#). A typical heat-wait-seek (HWS) method, described in detail by [Lei et al. \(2017\)](#), was employed to find the onset temperature of the exothermic reactions of the LFP cells, while adiabatic-like conditions were imposed during the TR event. The HWS method was set up with the following conditions: a start temperature of 50°C, end temperature of 315°C (the maximum operating temperature of the ARC), temperature step of 5°C, temperature rate sensitivity of 0.02°C min⁻¹ and a wait time of 60 min. The onset of self-heating of the cell is taken to be when the cell surface temperature rate is >0.02°C min⁻¹, while TR of the cell is taken to be when this rate is >1.0°C min⁻¹. The ARC test was carried out on LFP cells at 0%, 28%, 63%, 100% and 110% SOC.

The physical arrangement of the LFP cell in the ARC is depicted in [Figure 1\(b\)](#). The cell was removed from its shrink wrapping and an N-type thermocouple was attached to the surface of the cell with glass cloth tape. The cell was then suspended from an aluminium frame to ensure it did not come into contact with the walls of the ARC vessel. The cell was attached to the frame using glass cloth tape, to ensure that there was negligible heat transfer between the cell and frame, allowing the phi-factor to be taken as unity.

2.2. Flash Heating Test

The oven test was carried out using a *VWR DRY-Line 53* natural convection oven, shown in [Figure 1\(c\)](#), with a maximum operating temperature of 220°C. The oven was preheated to the desired abuse temperature before a cell (at 100% SOC) was placed on a steel wire shelf in the centre of the oven. With minimal surface to surface contact between the cell and the shelf, heat conduction from the shelf can be assumed to be negligible. The oven and cell surface temperatures were measured by K-type thermocouples and recorded using a *Pico USB TC-08* data logger. The shrink wrapping on the cell was removed to improve the contact between the thermocouples and cell surface. The test began from the moment the cell was placed in the oven and ran for 90 minutes. [Figure 1\(d\)](#) shows the placement of the thermocouples on the cell and in the oven. The two cell thermocouples were attached to the long edge of the cell

(i.e. not the flat end terminals) with glass cloth tape, 1 cm from either end of the cell. The thermocouple measuring the oven temperature was placed at the same height as the cell but away from the cell surface so that it was not affected by the heat generated by the cell. All cells were tested at 100% SOC and had been stored in ambient conditions beforehand.

3. Results and Discussion

3.1. Arc Test

The results of the ARC experiments are given in Figure 2 (where Figure 2(a) to Figure 2(e) are for cells at 100%, 110%, 63%, 28% and 0% SOC respectively) and the notation of R1, R2 and R3 in the key of the sub-plots is used to denote the individual test runs at each SOC. The sub-plots of Figure 2 show (for the cell surface) the rate of temperature increase at a given temperature during cell self-heating above the sensitivity value of $0.02^{\circ}\text{C min}^{-1}$. The experimental repeats for each SOC in the sub-plots of Figure 2 show that, for commercial cells, the exothermic behaviour is consistent between cells of same the SOC. This allows battery manufactures to be confident in the exothermic behaviour of one cell within a battery module/ pack. It should also be noted that all cells remained intact up to 315°C at all SOC. This implies that, with operational cells vents, the rate of gas generation was not great enough to lead to a build up of internal cell pressure that could cause the cell case to fracture and/ or explode.

Figure 2(a) shows the results of cells at 100% SOC and will be discussed first as a bench mark to compare the results at other SOC. It can be seen that from the onset of self-heating at 95°C , the temperature rate increases up to the maximum temperature rate of $3.7^{\circ}\text{C min}^{-1}$ (value determined from the average of the maximum temperature rates of the three runs) at $\sim 230^{\circ}\text{C}$, whereafter, the temperature rate generally reduces with increased temperature until the end of the experiment (315°C). A secondary peak of $1.6^{\circ}\text{C min}^{-1}$ is seen at 280°C . From Figure 2(a), we see that the cells temperature behaviour can be further split into 4 distinct regions, determined by inspection (also depicted in Figure 3 which, for visual clarity, compares a single ARC temperature rate plot from each SOC that is most representative of the average behaviour at each respective SOC): (I) first exotherm - containing self-heating onset to venting; (II) endothermic event - attributed to the expansion of the venting gases cooling the cell (and is seen in the as a break in the data points as the ARC exits exothermic mode); (III) second exotherm - containing the first peak temperature rate; (IV) third exotherm - containing the second peak temperature rate.

From the temperature rate plot in Figure 2(a), and referring to the onset temperature of the individual reactions from the literature discussed in the introduction, relevant reactions can be associated with each region. The first exotherm in region (I), over the range of $95\text{--}150^{\circ}\text{C}$ can largely be attributed to the solid electrolyte interphase (SEI) reaction, with an increasing contribution from the negative electrode-solvent (NE) reaction at higher temperatures.

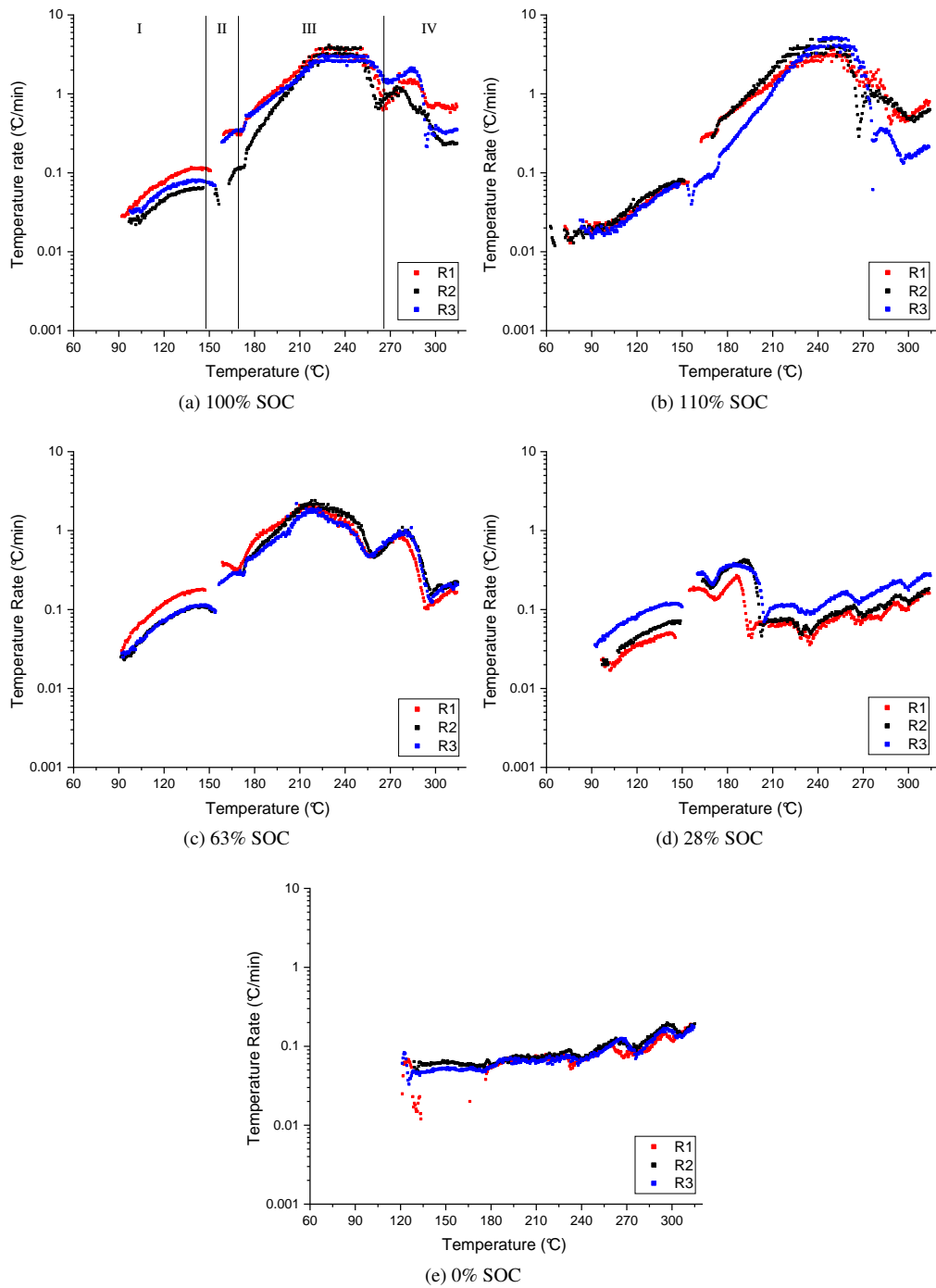


Figure 2: Cell surface temperature rate against cell surface temperature from exothermic period of HWS test for various SOC (note logarithmic scale on y-axis).

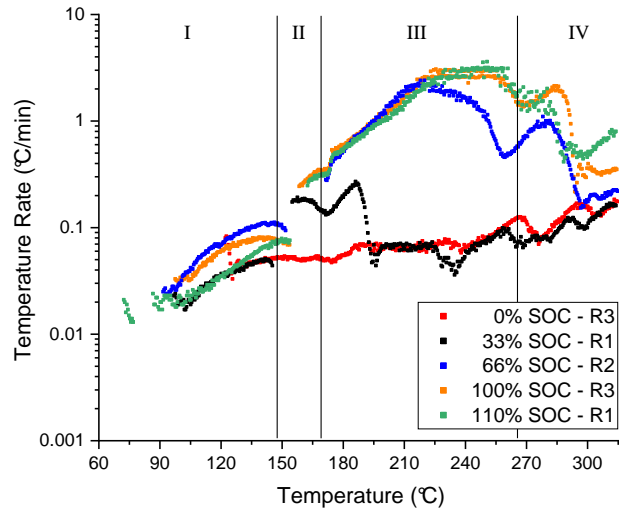


Figure 3: Comparison between SOC within ARC tests. Regions: (I) first exotherm - containing self-heating onset to venting; (II) endothermic event - due to venting; (III) second exotherm - containing the first peak temperature rate; (IV) third exotherm - containing the second peak temperature rate.

The second exotherm in region (III), over the range of 150–255°C is due to the NE and positive electrode-solvent (PE) reactions. The NE reaction generates the most heat overall, on the scale of an order of magnitude greater than the PE reaction (see Table 1), and therefore dominates the temperature rate profile in this region. The final exotherm in region (IV), at >255°C, is due to the increased contribution of the decomposition reaction of the electrolyte with oxygen evolved from the decomposition of the LFP.

From Figure 2(b) and Figure 2(c), it can be seen that the temperature rate profiles at 110% and 63% SOC respectively are similar to that at 100% SOC. However, as can be seen in Figure 3, there are two distinct differences when comparing the results from these three different SOC with regards to regions (III) and (IV): (1) the magnitude and position of the absolute peak temperature rate, and (2) the magnitude and position of the second temperature rate peak.

With regards to (1) and referring to Figure 4 that shows the absolute maximum cell temperature rates, the temperature at which the absolute maximum rates occur and self-heating onset temperature for a given SOC, it can be seen that as SOC increases the absolute peak temperature rate also increases. This occurs due to the greater amount of energy stored and the resulting increased instability of the electrodes at higher SOC, particularly in the negative electrode due to more lithium being available in the intercalated carbon to react with the binder, filler and electrolyte at higher temperatures (Roth and Doughty, 2004). This behaviour can also explain (2), as more heat generated over a large temperature range from the NE and PE reactions at 110% SOC leads to a greater overlap between these two reactions and the electrolyte reaction, and hence a summation of their heat generation rates. This in turn reduces the distinction between the 1st and 2nd peak temperature rates leading to an increase in the overall peak rate. Conversely,

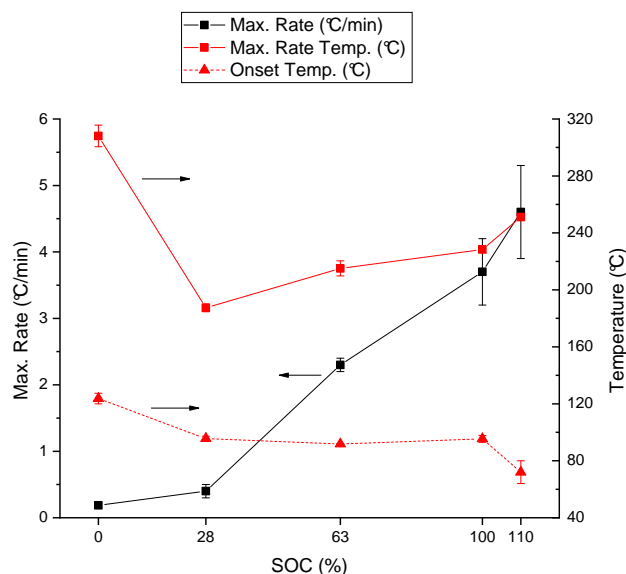


Figure 4: Maximum rate at given SOC with the corresponding temperature that the maximum rate occurs at; and onset temperature of first exotherm (Note: error bars are equal to one standard deviation).

at 63% SOC, the increased stability of the electrodes leads to less heat being produced over a smaller temperature range which in turn increases the separation between the 1st and 2nd peak rates. Additionally, the reduction in the 2nd peak temperature rate at 63% SOC compared to that at 100% SOC can be somewhat attributed to (1) the likelihood of less oxygen been available to fuel the electrolyte reaction as the positive electrode will have decomposed less, releasing less oxygen; and (2) the reduced contribution of the NE and PE reactions at higher temperature to the overall heat generated.

Figure 2(d) presents the ARC results at 28% SOC and shows the temperature rate increases from onset until a peak at $\sim 190^{\circ}\text{C}$ whereupon the rate drops. Between 200°C and 225°C , the temperature rate is relative constant, while after 225°C the temperature rate slowly increases. The behaviour in regions (I) and (II) is comparable to that for the 100% SOC, see Figure 3. However, the peak temperature rate in region (III) for the 28% SOC case occurs at a much lower temperature ($\sim 190^{\circ}\text{C}$) than at higher SOC and is present over a smaller temperature range. These characteristics suggest that the NE reaction is the main contributing factor to the self-heating peak, as the NE reaction is more unstable and energetic at lower SOC than the PE reaction. The behaviour beyond 200°C is due to the decomposition of the PE and electrolyte reactions; however, due to the stability of the cathode, these reactions do not occur at a significant rate.

Finally, Figure 2(e) presents the ARC results at 0% SOC and shows the temperature rate is relatively low across all temperatures with a slight trend of increased rate with temperature. The initial heating in region (I) is comparable to that of the other SOCs, see Figure 3, with the exception of a delay in the onset temperature. The peak temperature rate at $\sim 190^{\circ}\text{C}$ that occurs in the 28% SOC is no longer present, while after 200°C the temperature rate is similar to

that in the 28% SOC case. The loss of the temperature rate peak at $\sim 190^{\circ}\text{C}$ is consistent with the electrodes being in their most stable state and, with the negative electrode being fully delithiated, the NE reaction only occurs at a slow rate. As the cell is fully discharged, the heating from the PE electrode will be negligible (Takahashi et al., 2002). Additionally, as the discharged PE electrode will also have released very little O_2 , the electrolyte reaction will be limited, but might be facilitated by O_2 entering from the open vent (Belov and Yang, 2008). The factors causing the delayed onset are discussed later.

As stated previously, from Figure 4 we can see that, at increased SOC, the maximum temperature rate during TR is greater. Further, disregarding 0% SOC (because there is no distinct peak in the temperature rate plot of Figure 2(e)), the temperature at which these peak rates occur increases with SOC. However, it can also be seen that the increase in temperature rate is not linear, with a proportionally greater increase in maximum temperature rate over the range of 28%–100% SOC than 0%–28% SOC, and greater still over the range of 100%–110% SOC. Similar behaviour is seen by Refs. (Mendoza-Hernandez et al., 2015; Chen et al., 2015) in the study of LiCoO_2 and LiMn_2O_4 cells, as shown in Figure 5. This behaviour is related to the amount of energy stored, the stability of a given reaction at a given SOC and the extent to which reactions occur simultaneously. In other words, as SOC increases there is greater electrochemical potential energy that leads to higher reaction rates and more heat generation, while the resulting greater heat generation leads to larger temperature increases and hence the occurrence of more energetic reactions that only occur at higher temperatures in turn leading to peak reaction rates occurring at higher temperatures. As the maximum temperature rate is directly related to the maximum heat generation rate, it therefore is a good quantity by which to quantify safety, as one can use the maximum temperature rate at different SOC to predict the risk of TR at different SOC.

Figure 5 compares the maximum temperature rate at different SOC from the results in this work to that of different chemistries from the literature. Considering the 100% SOC case, it can be clearly seen that LFP cells have a significantly lower maximum temperature rate, of around 3 orders of magnitude lower, and hence are significantly safer than the other chemistries. Indeed, even at low SOC, LFP is significantly less reactive than LCO cells. Readers should note the different energy densities of the cells compared. The higher energy densities (2.2–3.3 Ah) of the NMC, LCO and NCA cells from the literature makes direct comparison difficult against the LFP (1.5 Ah) studied here. However, as the LMO literature case with a capacity of 1.6 Ah clearly shows, it is not the amount of energy available within a cell that is the major concern for maximum temperature rate, but the cell's chemistry and the resultant reaction rates of its components.

Figure 4 also shows the relationship between onset temperature and SOC. Between 28% and 100% SOC, there is little difference in the onset temperature which occurs between 92 – 96°C . However, at 0% SOC and 110% SOC, there is a significant delay (127°C) to and advance (67°C) of, respectively, the onset temperature. The delay to onset at

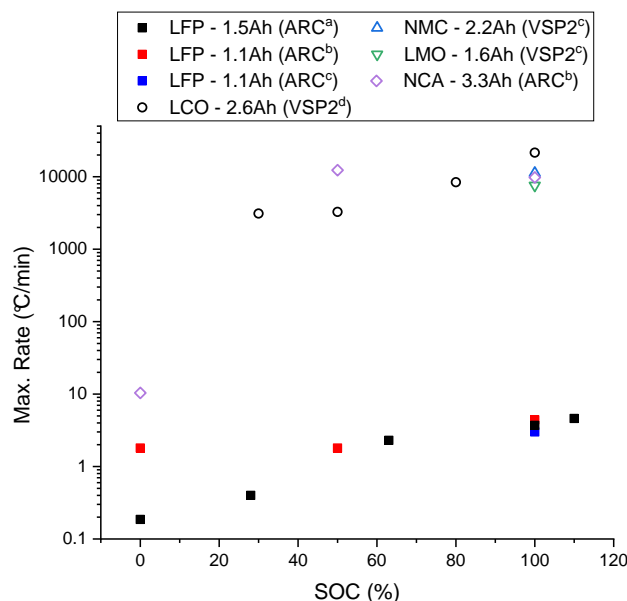


Figure 5: A comparison of maximum temperature rates at given SOC for 18650 cells of different chemistries, nominal capacities at 100% SOC are given. ^aThis work. ^b(Kvasha et al., 2018). ^c(Lei et al., 2017). ^d(Chen et al., 2015).

0% SOC suggests that there is a reaction other than the SEI decomposition contributing to the onset of self-heating in region (I) of Figure 3 for cells at higher SOC. This is because, once formed, the SEI layer is metastable (Verma et al., 2010; An et al., 2016) and hence would decompose and produce the same amount of heat irrespective of SOC. Under the assumption of a four reaction system, this suggests that the lithiation of the negative electrode at SOC $\geq 28\%$ causes a reduction in the onset temperature. To the authors' knowledge, this is the first report of the negative electrode to be the trigger of thermal runaway. This offers the opportunity to design batteries where electrodes are thermally decoupled.

The mechanism that advances the onset temperature at 110% SOC is easily identified. Upon overcharge, lithium is irreversibly removed from the cathode and deposited on the surface of the anode. Upon heating, the delithiated cathode and/or the deposited lithium metal leads to reduction of the electrolyte at relatively low temperatures, below that of the NE or SEI reactions and hence leads to a reduction of the onset temperature of self-heating (Ohsaki et al., 2005; Tobishima and Yamaki, 1999; Zhang, 2014).

Figure 6 presents a thermal map of the ARC data from Figure 2, and in this format allows for an easier assessment of the TR processes at different SOC. The green region represents the temperatures over which no detectable self-heating occurs and the ARC is operating in HWS mode. There is an exception at approximately 150°C, due to the cooling of the cell by vented gases which dissipates more heat than is generated by the decomposition reactions. The orange and red regions of Figure 6 indicate when the ARC is in exothermic mode and the cell is under going

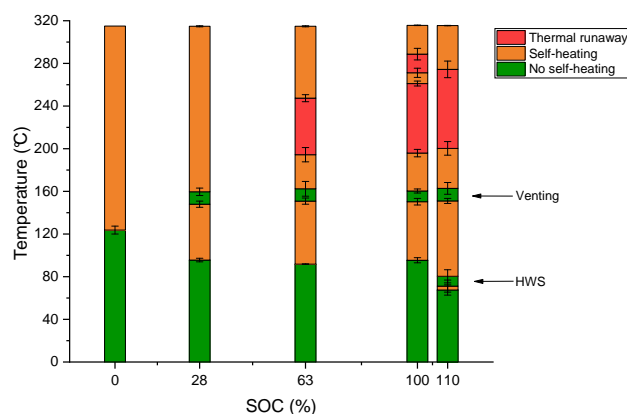


Figure 6: Thermal mapping as a function of SOC. No self-heating when temperature rate is $<0.02^{\circ}\text{C min}^{-1}$, self-heating when temperature rate is $>0.02^{\circ}\text{C min}^{-1}$, and thermal runaway when temperature rate is $>1^{\circ}\text{C min}^{-1}$. (Note: error bars are equal to one standard deviation.)

self-heating (orange) or TR (red).

As can be seen from Figure 6, the venting of gasses at 150°C only occurs in cells of 28–110% SOC, with the exception of run R1 of 0% SOC. It can be assumed that venting does not occur at 0% SOC due to the stability of the cell, leading to little decomposition of the electrodes/ electrolyte and hence little gas production. Also, once self-heating has been initiated, the reactions are self sustaining up to the ARC cut off temperature. This is evident of no further HWS procedure been carried out by the ARC from the onset of self-heating until the end of the test. This is excluding the 110% SOC case, where for runs R1 and R2 there is an initial self-heating reaction at $\sim 67^{\circ}\text{C}$ due to the lithium plating decomposition reaction (Ohsaki et al., 2005; Tobishima and Yamaki, 1999; Zhang, 2014) before self sustaining self-heating is initiated at $\sim 75^{\circ}\text{C}$. At 110% SOC the onset temperature of self-heating is therefore 75°C . This is still lower than the other SOC cases, hence overcharge is still a cause of reduced stability, and therefore a safety concern, in LFP cells. Analysis of the TR region, indicated in red in Figure 6, shows that at 28% SOC and below TR does not occur, while in all other cases TR occurs at temperatures $>200^{\circ}\text{C}$. As TR onset occurs at temperatures $>200^{\circ}\text{C}$, and the NE reaction onset occurs at temperatures as low as 80°C (Richard and Dahn, 1999b; MacNeil et al., 2000) while the PE reaction onset does not occur until 180°C (Jiang and Dahn, 2004b,a), it implies that the NE reaction is the cause of TR initiation as the PE reaction will only have just initiated and have a negligible heating rate. Hence, if the carbon anode self-heating onset can be postponed, then LFP cells can be stable to greater temperatures.

3.2. Flash Heating Test

After undergoing an oven test, visual inspection of the LFP cells show that the cells remain intact even after a TR event has occurred and hence do not present an explosion risk. The only visible difference between the 180°C and 220°C oven temperature cases is that the higher oven temperature leads to a cell that has a greater area of

darker discolouration around the cell vents. This is attributable to a greater amount of decomposition/ combustible products being produced and expelled through the cell vents.

Figure 7 shows the resulting cell surface and oven temperatures for the oven tests in which Figure 7(a) and Figure 7(b) present the results from oven set temperatures of 180°C and 220°C respectively. The notation R1.x, R2.x etc. in the key of the sub-plots in Figure 7 is used to denote the individual oven test runs for the respective sub-plot i.e. x = a,b. This is done for ease of reference when analysing the results of the two oven set temperatures in the following discussion. In both Figure 7(a) and Figure 7(b), it can be seen that there is an initial drop in oven temperature before returning to the oven set temperature. The temperature drop is due to cooling during oven chamber access. This means that, even though the cells are placed into a preheated oven, the oven set temperature is not precisely the temperature experienced by the cell. However, as the oven temperature is recorded independently, an accurate reading of the oven temperature is obtained and only varies slightly between experimental runs (see Figure 7). Additionally, as the heating of the cell prior to TR is most important to the behaviour of the TR event, the oven temperature the cell experienced is taken as the average oven temperature up to the occurrence of maximum cell surface temperature. In this manner, for the four experimental repeats at each oven set temperature, the mean oven temperature for the 180°C case was 180°C, with a relative standard deviation (RSD) of 0.43%, while, for the 220°C case, it was 215°C, with a RSD of 0.97%.

The cell surface temperature plots in Figure 7 show the increase in cell surface temperature from room temperature up to a maximum temperature beyond the oven temperature, before returning to the oven temperature. This behaviour can be broken into four regions. Region (A) is below a cell surface temperature of 95°C, corresponding to the onset temperature of self-heating reactions determined from the ARC data of a cell at 100% SOC in Subsection 3.1. Region (B) is a period of increasing reaction rates and self-heating over a cell surface temperature range of 95°C to 175–180°C, at which point venting occurs. Region (C) is the period of TR, from venting to peak temperatures. Finally, Region (D) is the period at which the cells cool down to the oven temperature after the reactions have finished.

It can be seen from Figure 7 that, along with the high repeatability of the oven temperatures, there is also a high degree of repeatability for the measured surface temperatures between each experimental run. Disregarding the clear outliers (to be discussed later) for each oven temperature (R1.a and R3.b of the 180°C and 220°C cases respectively) the mean values of the maximum cell surface temperature and time to maximum temperature from Figure 7 are presented in Table 2. From this data, it can be seen that these maximum cell surface temperatures relate to a temperature rise of 46°C and 182°C above the mean oven set temperatures of 180°C and 215°C respectively. From the data presented here, compared to that from the literature (Tobishima and Yamaki, 1999; Hatchard et al., 2001), we can see that LFP cells are much safer than LCO cells for a given oven temperature. LFP cells, compared to LCO, are more stable as they go into rapid TR at a higher oven temperature (200°C compared to 155°C), and react

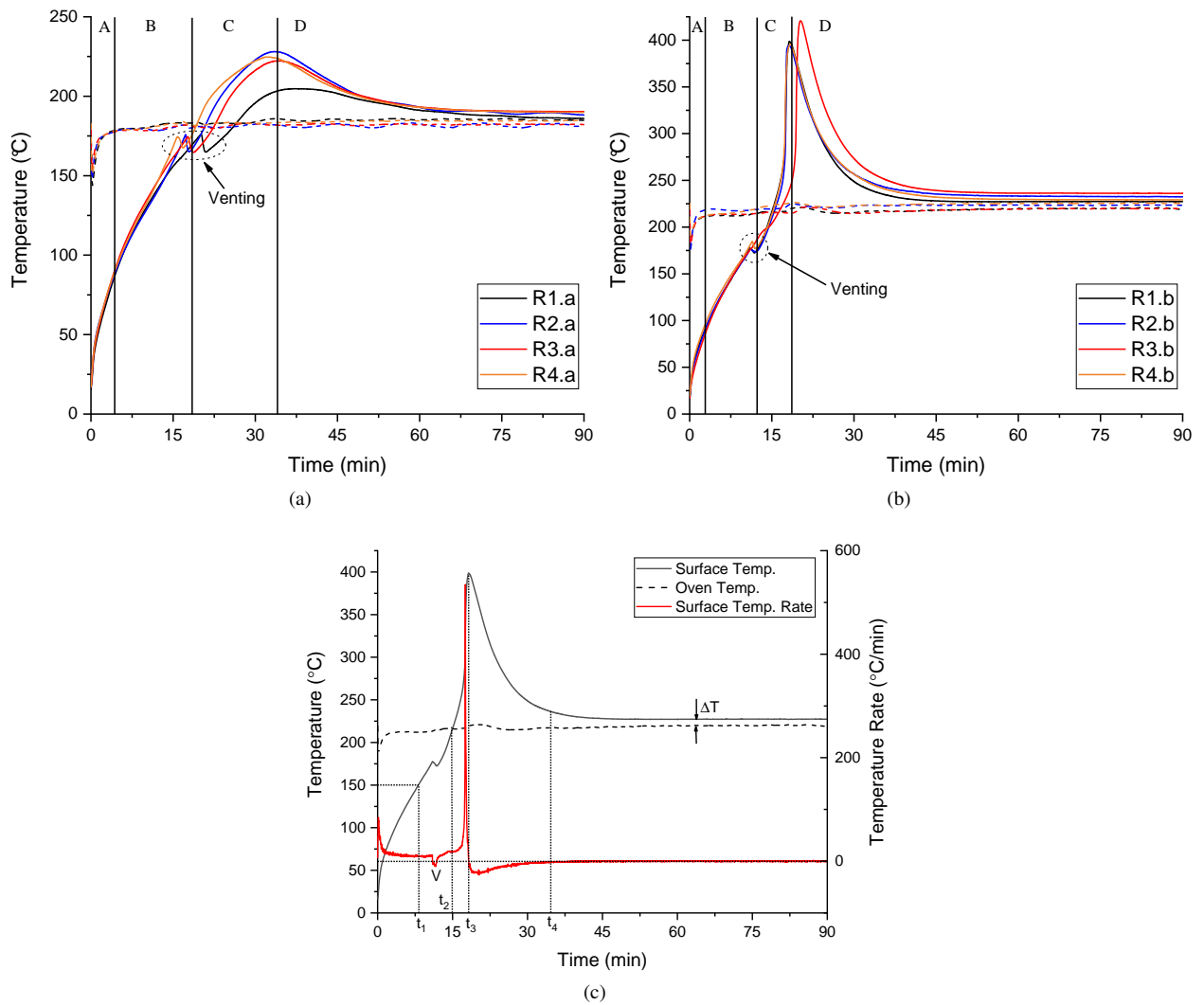


Figure 7: Cell surface temperature (solid line) as a result of been placed in an oven set to (a) 180°C and (b) 220°C (Dashed line denotes oven temperature). Regions (A) cell surface temperature <90°C - heating by convection only, (B) cell surface temperature >90°C - heating with increasing contribution from self-heating, (C) thermal runaway - moderate in (a), severe in (b) and (D) cooling. (c) An example of the cell surface temperature rate (R1.b) with key time instances.

Table 2: Mean values of important measurements for each oven set temperature.

Oven set temperature (°C)	Calculated oven temperature (°C)	RSD (%)	Max cell surface temperature (°C)	RSD (%)	Time to max temperature (min)	RSD (%)	Max temperature rate (°C min ⁻¹)	RSD (%)
180	180	0.43	226	0.94	33	3.44	-	-
220	215	0.97	396	0.46	18	0.45	616	27

less severely leading to lower maximum temperatures (~400°C compared to ~700°C).

From the previous discussion we see that these LFP cells under a free convection oven test procedure behave in a similar manner to those of other chemistries in literature (Tobishima and Yamaki, 1999; Hatchard et al., 2001; Jiang et al., 2004), i.e a higher oven set temperature leads to a higher cell TR temperature in a shorter amount of time, as well as reducing the time to venting (see Table 2). Even though the venting occurs sooner at higher oven temperatures, it occurs at a similar cell temperature for each oven set temperature. Therefore, we assume it relates to cell internal pressure and hence as a result of greater convection heating and of faster reaction rates for the decomposition reactions which in turn leads to gas being produced more quickly.

Although the difference in maximum surface temperatures between the two oven temperatures is to be expected, it is interesting to note the large increase in cell surface temperature rate of the 220°C oven case. This suggests that between the two oven temperatures there are additional reactions occurring in the 220°C case compared to the 180°C case. The analysis of the ARC data for a LFP cell at 100% SOC in Figure 2(a) shows peak reaction rates to be at 228°C, while the decomposition of the LFP electrode has peak reaction rates at temperatures >210°C (Yamada et al., 2001; MacNeil et al., 2002; Takahashi et al., 2002; Jiang and Dahn, 2004b) and heating due to electrolyte decomposition does not occur until >255°C (Chen and Richardson, 2010; Ben Mayza et al., 2011). Therefore, in the 180°C case where the cells surface temperature did not reach beyond 230°C, it is clear the cell's internal temperature does not reach a temperature that leads to the onset, or to significant reaction rates, of one or both of the PE and, electrolyte reactions. Most significantly, the cells in the 180°C case did not reach the point for the evolution of oxygen and the electrolyte reaction. The absence of these reactions therefore leads to the significantly reduced reaction rate and heat of reaction of the cell for the lower oven temperature.

Furthermore, Figure 8 shows the resulting maximum cell surface temperatures and maximum cell-oven temperature difference (ΔT) occurring at particular average oven temperatures before TR, with additional oven temperatures besides the 180°C and 220°C cases presented so far. It can be seen that, between 170°C and 190°C, there is a slight increase in maximum cell temperature with oven temperature and, between 190°C and 200°C, there is a step increase in maximum cell temperature. Beyond 200°C oven temperature, there again is only a slight increase in maximum cell temperature. The temperature difference (ΔT) is almost flat below 190°C and above 220°C oven temperatures. However, between a (pre-TR average) oven temperature of 190°C and 200°C (denoted by the red highlighted region

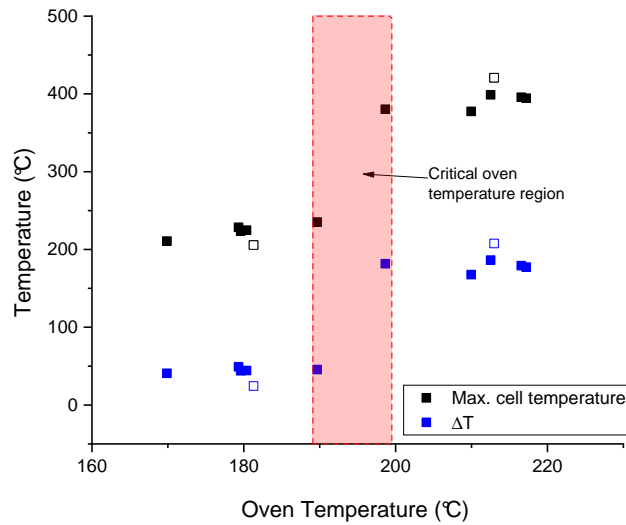


Figure 8: Cell Surface Temperature Vs Oven Temperature. (Black, filled) maximum cell surface temperature due to oven set temperature. (Black, unfilled) lower left and upper right, denote outliers R1.a and R3.b respectively. (Blue, filled) Maximum increase in cell surface temperature above oven set temperature, (Blue, unfilled) outliers as before. Red shaded region indicates the oven temperature range over which there is a step change in resultant cell surface temperature. (Note: oven temperature values are those calculated to be the average oven temperature before maximum cell temperature.)

in Figure 8), there is a significant increase in the observed ΔT suggesting that, in this oven temperature range, the cell reaches the critical temperature for the additional (PE, electrolyte) reactions to occur. This indicates that, if an LFP cell is maintained below this critical temperature for these reactions, then, not only will the overall cell temperature from TR be considerably lower, but the rate of reaction of the cell will be much lower and therefore the cell much easier and safer to manage.

By comparing the oven data to the ARC data at 100% SOC, we see that for cells exposed to an oven temperature of 220°C, a more drastic TR event occurs compared to the ARC tests, similar behaviour is noted by Lei et al. (2017). In the oven test, maximum cell surface temperatures of ~400°C are reached with maximum temperature rates of 616°C min⁻¹ (see Table 2), while, in the ARC tests, the maximum cell surface temperature (315°C) and temperature rates (4.1°C min⁻¹) are significantly lower, even though there is no heat loss. This can be explained by the contribution of self-heating to cell temperature rise. In the ARC, the temperature rise of the cell is entirely due to the thermal energy generated by self-heating, raising the cell's temperature from 95°C to 315°C. In the oven, however, due to rapid convective heating from the air and conduction through the cell, the cell can reach a higher temperature (up to the oven set temperature) more quickly than that which would occur from the evolution of the reaction rates alone. As the cells (at 100% SOC) are identical in the oven and ARC tests, the amount of energy that can be released during TR will also be the same. However, in the oven test, due to the relatively high temperature rate from convection heating (compared to self-heating in ARC at same temperature), there is a significant increase in temperature before

the decomposition reactions can progress. Hence more heat is released at higher temperatures (compared to the ARC), in turn leading to a larger temperature rise over all. Additionally, the compounding of the reaction rates of the four reactions at higher temperatures leads to an overall increase in reaction rate of the cell. Moreover, for the oven at 220°C, it can be seen that TR initiates below the oven set temperature and occurs so rapidly that the system is effectively adiabatic. This indicates that the severity of TR is increased under rapid heating of the cell and should be taken into account when considering safety, especially in circumstances such as rapid heating of a cell due to short circuit of a neighbouring cell or overheating due to temperature control failure or another source of heat such as fire.

Figure 7 also shows that, with the exception of run R3.b, the LFP cells vent at approximately 175°C resulting in a 5–10°C temperature drop at the cell's surface. However, with regard to the cell in R3.b that does not show this temperature drop, there is an inflection in the cell's temperature profile a few minutes after venting for the other three runs (R1.b, R2.b & R4.b) within the 220°C case. This inflection indicates that there is a reduction in the net heat generated, which in-turn implies that the cell's vents opened, but not completely. It is this lack of successful venting, and hence cooling of the cell by the Joule-Thomson effect, to which we attribute the 24°C increase in maximum cell temperature of R3.b compared to the mean maximum temperature of runs R1.b, R2.b and R4.b. This shows that, although venting is not capable of halting TR, venting does influence the maximum temperature reached.

With regards to R1.a, the cell used in this run had a capacity of 1495 mAh compared to the mean value of 1478 mAh for the cells of all four runs of the 180°C case. It was exposed to the highest oven temperature, 181°C compared to the mean of 180°C and had a temperature drop due to venting in the same range as R2.a and R3.a. Such factors can be ruled out as been influential to the temperature difference between R1.a and the remaining runs in 180°C case. Hence, one can speculate that the cause of this anomaly is due less heat been produced due to decomposition reactions not fully completing. This and the previous paragraph show the importance of considering cell variability when study the safety of battery modules or packs.

A conservative comparison of the oven simulation data from (Peng and Jiang, 2016) to this newly gathered oven experimental data, shows that, in simulation, there is a large overestimation of the oven temperatures that lead to TR, a large underestimation of cell temperature increase due to TR and an overall disagreement with the qualitative behaviour of the cell surface temperature profile. This outlines the importance of these oven exposure results as a data set for validation of TR models of LFP cells.

3.3. Comparison of Heat Release Under Different Abuse Scenarios

For further insight in to the reactions taking place under the different abuse scenarios, an analysis of the heat released by cells at 100% SOC under ARC and oven testing was undertaken.

Under ARC the thermal energy released can be easily calculated from the adiabatic temperature rise of the cell

by Equation 2. In Equation 2, the adiabatic temperature (ΔT) is the difference between the onset and maximum cell temperature, C_p is the average specific heat of the cell and m is the average mass of the cell. The mass of the cell was measured to be 40.48 g. The C_p value, following the method outlined by Bryden et al. (2018), was calculated by Equation 3 from the average temperature rate (dT/dt) of a cell in an adiabatic environment subject to a constant heating power (P) at the cells surface. The specific heat of the cell was determined to be $1107 \text{ J kg}^{-1} \text{ K}^{-1}$. For the cells at 100% SOC under ARC, the average adiabatic temperature rise is approximately 220°C . Therefore, from Equation 2, $Q_{ARC} = 9.85 \text{ kJ}$.

$$Q = \Delta T C_p m \quad (2)$$

$$P = \frac{dT}{dt} C_p m \quad (3)$$

The determination of the heat released under oven exposure can be estimated from the cell surface temperature rate, Figure 7(c) shows an example cell surface temperature rate plot from oven exposure. The temperature rate, determined by differentiation of the temperature plot, can be used in conjunction with Equation 3 to determine the heating power at the cells surface for every instance in time. By integration, this in turn can be used to determine the thermal energy released during TR.

As the temperature, and in turn the temperature rate, are both dependent on the heat transfer from the oven as well as the self-heat generation, their contributions to cell heating have to be identified. As discussed in the ARC study, self-heating does not initiate until $\sim 95^\circ\text{C}$, so at any point in time where the cell surface temperature is $< 95^\circ\text{C}$ it can be confidently said that transfer from the oven dominates. Although a large temperature difference between the cell interior and cell surface can exist during TR due to internal heat generation, at this early stage with no self-heating the surface can be assumed to be hottest (Parhizi et al., 2017). Above this temperature, self-heating will become increasingly important. On inspecting the temperature rate (taking the profile in Figure 7(c) as an example), it is found that after a plateau in the rate, the rate increases at times coinciding with cell surface temperatures greater than approximately 150°C . Hence, it is assumed that self-heating is not important until surface temperatures are $> 150^\circ\text{C}$, at which point it dominates the heat rise of the cell up to the cell's maximum temperature. Beyond the maximum temperature the cell cools. However, this does not mean the decomposition reactions are complete at this point. This is evident from the temperature difference between the cell surface and oven at the end of the test, suggesting low rate reactions are still occurring such that the cell does not equilibrate at the oven temperature.

From this interpretation several key time instances and features can be identified and utilised to estimate the heat

generated during TR of a cell under oven exposure. The time instances t_1 , t_2 , t_3 and t_4 , depicted on [Figure 7\(c\)](#), can be defined as: t_1 , the time that self-heating becomes dominant; t_2 , the time that the cell becomes hotter than the oven; t_3 , the time that the maximum cell temperature occurs and the point the cell begins to cool; and t_4 , the point that the cell temperature rate is negligible. Beyond t_4 the temperature difference between the oven and cell surface (from t_4 to the end of the test) is defined as ΔT_{t_i} , at t_i . The negative rate region at point V is due to cooling from the venting gases.

The absolute energy released by self-heating (i.e. considering heat loss due to venting as positive as it inherently originates from self-heating) between t_1 and t_3 , $Q_{t_1-3,Abs}$, can be determined by integrating the absolute power between t_1 and t_3 . In turn the energy lost through venting, Q_V , can be estimated from the difference between $Q_{t_1-3,Abs}$ and the net energy released between t_1 and t_3 , $Q_{t_1-3,Net}$, i.e. $Q_V = Q_{t_1-3,Abs} - Q_{t_1-3,Net}$. If no heat is generated after the peak temperature, it is expected that the heat lost during t_3-t_4 , $Q_{t_3-4,Loss}$ (by the cell cooling down to the oven set temperature), to be equal to the heat that was generated between t_2-t_3 , Q_{t_2-3} . Any difference in these values can be attributed to self-heating as the cell cools. Hence, the heat generated as the cell cools is defined as, $Q_{t_3-4} = Q_{t_2-3} + Q_{t_3-4,Loss}$, as $Q_{t_3-4,Loss}$ is inherently negative. Beyond t_4 , where $dT/dt \approx 0$, we can assume steady state conditions. Hence, the self-heating rate, $P_{t_i,SH}$, equals the heat loss rate due to convection and radiation, $P_{t_i,HL}$, at each interval in time t_i between t_4-t_{end} . Radiation is considered because [Hatchard et al. \(2000\)](#) highlights its importance in convection oven experiments. The heat loss, $P_{t_i,HL}$, is defined by [Equation 4](#), where T_C and T_O are the cell surface and oven temperature respectively, h is the convective heat transfer coefficient, A is the heat transfer area, ε radiative heat transfer coefficient and R is the Stefan-Boltzmann. Therefore, the heat generated is determined by [Equation 5](#), where Δt_{t_i} is the time interval between data points. The total heat generated by self-heating is given by [Equation 6](#).

$$P_{t_i,HL} = (T_{C,t_i} - T_{O,t_i}) hA + (T_{C,t_i}^4 - T_{O,t_i}^4) \varepsilon AR \quad (4)$$

$$Q_{t_4-end} = \sum_{t_4}^{t_{end}} P_{t_i,HL} \Delta t_{t_i} \quad (5)$$

$$Q_{Oven} = Q_{t_1-3,Abs} + Q_{t_3-4} + Q_{t_4-end} \quad (6)$$

Following this method, with $h = 10 \text{ W m}^{-2} \text{ K}^{-1}$ (estimated from [\(Hatchard et al., 2001\)](#) from the values for a bare stainless steel cylinder, $12.5 \text{ W m}^{-2} \text{ K}^{-1}$, and for a cell with a label, $7.2 \text{ W m}^{-2} \text{ K}^{-1}$, h for the tested cell is calculated to be the average of these values assuming half of the cell surface area is bare stainless steel, and the remaining surface that is covered in glass cloth tape has the same h if was covered in the label), $A = 4.18 \times 10^{-3} \text{ m}^2$,

Table 3: Heat released during TR by cells under oven exposure

Oven Temperature [°C]	$Q_{t_1-3, Abs}$		$Q_{t_1-3, Net}$		Q_{t_2-3}		$Q_{t_3-4, Loss}$		Q_{t_4-end}		Q_{Oven}		Q_V	
	[kJ]	SD.	[kJ]	SD.	[kJ]	SD.	[kJ]	SD.	[kJ]	SD.	[kJ]	SD.	[kJ]	SD.
180 (ave. R2.a-R4.a)	4.21	0.27	3.38	0.12	2.00	0.12	-1.59	0.16	0.32	0.22	4.94	0.42	-0.83	0.19
180 (outlier R1.a)	3.37	-	2.41	-	0.94	-	n/a	-	n/a	-	3.37	-	-0.96	-
220 (ave. R1.b, R2.b, R4.b)	11.54	0.20	11.03	0.10	7.90	0.25	-7.39	0.24	2.60	1.02	14.66	1.03	-0.51	0.18
220 (outlier R3.b)	12.12	-	12.12	-	9.20	-	-8.20	-	5.68	-	18.80	-	0.00	-

$\varepsilon = 0.8$ (Hatchard et al., 2001) and $\Delta t = 1$ s, the self-heat generated during TR under oven exposure is calculated and presented in Table 3. As can be seen from Table 3, the heat released (Q_{Oven}) by the cell exposed to the lower oven temperature is approximately a third of that at the higher oven temperature. This supports the previous statement in the discussion above, that at the higher oven temperature additional reactions, i.e. PE and electrolyte, are taking place. The amount of heat calculated to be released upon venting is greater in the lower oven temperature case. This is thought to be due to, in the higher oven temperature case, greater heat generation rates at the time of venting reducing the overall temperature reduction, in turn reducing the calculated heat loss. Additional to the temperature differences in the outlining results, compared to the respective temperature profiles for each oven case, the calculated heat released also indicates that a consideration regarding the safety of cells has to be made regarding the variability of heat released during TR of commercial cells, which are manufactured to be identical, when exposed to the same abuse conditions.

When comparing the two abuse methods, ARC and oven exposure, it can be seen that the cells under ARC generate significantly less heat ($Q_{ARC} = 9.85$ kJ) than cells exposed to oven temperatures of 220°C, which generate $Q_{Oven, 220^\circ C} = 14.66$ kJ of heat. The higher temperature oven clearly represents a more complete TR event when compared to the electrochemical energy available, $Q_{Elechem} = 17.28$ kJ (considering the cell under investigation has a capacity of 1.5 Ah at 100% SOC and a nominal voltage of 3.2 V). It is expected that a cell under adiabatic conditions in the ARC would capture the complete TR process, and hence the heat generated by the cell would be at least equal to that in the higher temperature oven case. As this is not the case, and as the ARC used here only operates up to 315°C, it is apparent that the ARC does not capture the TR event to completion.

In ARC, self-heating is defined when the temperature rate of the cell is $>0.02^\circ C \text{ min}^{-1}$. Naturally, self-heating can be defined as ending when the temperature rate drops below this value. Returning to the temperature rate plot of from the ARC test (Figure 2(a)), it can be clearly seen that the cell is some way off from this cut-off value. In fact the rate is almost constant from 300°C to the end, again suggesting an incomplete reaction. However, under similar (ARC) conditions but up to higher maximum operating temperatures, i.e. $>400^\circ C$ as this is what is reached in the oven test, it maybe seen that the cell reaches the same maximum temperature and generate the same heat release as in the higher oven temperature case. Also, the ARC been limited to a maximum temperature of 315°C also prevents determining if the cells at different SOC cease self-heating at different temperatures, and hence prevents determination of an accurate

heat release for different SOC. As this investigation is beyond the scope of the study here, it is recommended that the self-heating behaviour in an adiabatic environment, up to and above the maximum temperatures determined from the oven test, to be made the focus of future work, along with investigation to identify if the discrepancies between ARC and oven are true of other cell chemistries.

In contrast, the oven exposure test, with a set temperature high enough to induce rapid TR (in this case temperatures $>200^{\circ}\text{C}$), captures nearly the entirety of the decomposition process within the cell, in terms of the proportion of the electrochemical energy released as heat. Also, oven testing is cheaper and more readily accessible as a safety test. Hence, we conclude that ARC alone could be unsuitable for characterising TR as it does not capture the full severity of TR (in terms of temperature rate), while it also may not capture maximum achievable cell temperatures, and, as such, should be complemented with oven testing. However, as the temperature measurements are recorded with thermocouples on the cell's surface, there will be a lag between the reactions occurring and the measured temperature. This could have implication on differentiating the individual chemical decompositions reactions compared to ARC, particularly during the high-rate thermal processes that occur during TR. To supplement this, the use of TR abuse modelling could be used to predict the decomposition reaction process and self-heat generated during oven testing, whilst also checking the assumptions of the simple model used here to determine the self-heat generation in the oven test. However, this is beyond the scope of this paper, and the topic of future work.

4. Conclusion

Accelerated rate calorimetry and free convection oven experiments were undertaken to investigate the stability and severity of TR in LFP cells. In both experiments, all cells remained intact, showing that LFP cells are likely to present no explosion risk.

Accelerated rate calorimetry was carried out on LFP 18650 cells at various states of charge, including overcharge. It was found that, as SOC increases, so does TR severity whilst cell stability reduces. From the resulting exothermic data, the contribution of the four decomposition reactions to the thermal runaway potential of the cell for each different SOC was discussed. To date, analysis of this type has not been presented in the literature. It was found that, at higher states of charge, there was an increasing overlap in the occurrence of the NE, PE and electrolyte reactions leading to an overall increase in maximum temperature rate. Also, the main contributions to TR at SOC of 100% and 110% were the negative and positive electrode reactions, while at lower SOC TR is dominated by the negative electrode reaction. At SOC greater than 0%, the negative electrode reaction is a significant contributor to self-heating onset temperature, and at 110% SOC, the lithium plating reaction reduces the onset temperature. At and below 28% SOC thermal runaway did not occur and hence is most suitable for the storage and transport of LFP cells, while for cells above 28% SOC the onset of TR occurs at approximately 200°C , at which point TR onset was due to the NE reaction.

In comparison to other chemistries studied in the literature, LFP cells have a reaction rate 3 orders of magnitude lower, even at low SOC, due to the limited oxygen production.

Oven tests were carried out to analyse the TR response of LFP 18650 cells at 100% SOC to understand how the cells respond under rapid heating, and to compare effects of the two different thermal abuse techniques on the severity of TR. It was shown that, for higher oven temperatures, the LFP cell had a more extreme TR event. Results indicate that if the cell temperature remains below the critical temperature (190–200°C) for cathode decomposition and electrolyte/O₂ reactions to occur, there is a significant reduction in maximum cell temperature and cell reaction rate, and hence an improved ability to manage the temperature rise of the cell, increasing overall safety. Compared against the literature, the LFP cells studied here are safer at a given oven temperature than other chemistries, with TR onset occurring at a higher oven temperature whilst reaching a lower maximum temperature. In oven tests, higher cell temperatures and temperature rates can be achieved than in ARC, showing how failure accelerated by external heating (where decomposition reactions are compounded) leads to more severe TR.

By comparing the heat released in both ARC and oven tests, it is shown that ARC (at temperatures up to 315°C) does not capture the full decomposition process of a cell during TR. Hence, care should be taken when determining safety from ARC results, while we recommend complementing ARC with oven testing, which presents a more severe TR event, to obtain a more complete picture of TR and cell safety.

It was shown that this work is important to computational research of TR in LFP 18650 cells by providing an essential data set useful for validation of models.

Conflicts of interest

There are no conflicts to declare.

Acknowledgements

The authors gratefully acknowledge the financial support of the Engineering and Physical Sciences Research Council (EPSRC) in the form of the Energy Storage and its Applications Centre for Doctoral Training (EP/L016818/1). We also thank Dr Eddie Cussen (The University of Sheffield), to whom we discussed our work and through which has led to an improved manuscript, although they may not agree with all of the interpretations/conclusions of this paper.

References

References

- Abraham, D.P., Roth, E.P., Kostecki, R., McCarthy, K., MacLaren, S., Doughty, D.H., 2006. Diagnostic examination of thermally abused high-power lithium-ion cells. *Journal of Power Sources* 161, 648–657. doi:[10.1016/j.jpowsour.2006.04.088](https://doi.org/10.1016/j.jpowsour.2006.04.088).
- An, S.J., Li, J., Daniel, C., Mohanty, D., Nagpure, S., Wood, D.L., 2016. The state of understanding of the lithium-ion-battery graphite solid

- electrolyte interphase (SEI) and its relationship to formation cycling. *Carbon* 105, 52–76. doi:10.1016/j.carbon.2016.04.008, arXiv:9809069v1.
- Belharouak, I., Sun, Y.K., Lu, W., Amine, K., 2007. On the Safety of the $\text{Li}_4\text{Ti}_5\text{O}_{12}/\text{LiMn}_2\text{O}_4$ Lithium-Ion Battery System. *Journal of The Electrochemical Society* 154, A1083. doi:10.1149/1.2783770.
- Belov, D., Yang, M.H., 2008. Failure mechanism of Li-ion battery at overcharge conditions. *Journal of Solid State Electrochemistry* 12, 885–894. doi:10.1007/s10008-007-0449-3.
- Ben Mayza, A., Ramanathan, M., Radhakrishnan, R., Ha, S., Ramani, V., Prakash, J., Zaghib, K., 2011. Thermal Characterization of LiFePO_4 Cathode in Lithium Ion Cells. *ECS Transactions* 35, 177–183.
- Bryden, T.S., Dimitrov, B., Hilton, G., León, C.P.D., Bugryniec, P., Brown, S., Cumming, D., Cruden, A., 2018. Methodology to determine the heat capacity of lithium-ion cells. *Journal of Power Sources* 395, 369–378. doi:10.1016/j.jpowsour.2018.05.084.
- Bugryniec, P.J., Davidson, J.N., Brown, S.F., 2018. Assessment of thermal runaway in commercial lithium iron phosphate cells due to overheating in an oven test. *Energy Procedia* 151, 74–78. doi:10.1016/j.egypro.2018.09.030.
- Chen, G., Richardson, T.J., 2010. Thermal instability of Olivine-type LiMnPO_4 cathodes. *Journal of Power Sources* 195, 1221–1224. doi:10.1016/j.jpowsour.2009.08.046.
- Chen, W.C., Li, J.D., Shu, C.M., Wang, Y.W., 2015. Effects of thermal hazard on 18650 lithium-ion battery under different states of charge. *Journal of Thermal Analysis and Calorimetry* 121, 525–531. doi:10.1007/s10973-015-4672-3.
- Doughty, D., Roth, E.P., 2012. A General Discussion of Li Ion Battery Safety. *The Electrochemical Society Interface* 21, 37–44.
- Feng, X., Ouyang, M., Liu, X., Lu, L., Xia, Y., He, X., 2018. Thermal runaway mechanism of lithium ion battery for electric vehicles: A review. *Energy Storage Materials* 10, 246–267. doi:10.1016/j.ensm.2017.05.013.
- Golubkov, A.W., Fuchs, D., Wagner, J., Wiltsche, H., Stangl, C., Fauler, G., Voitic, G., Thaler, A., Hacker, V., 2014. Thermal-runaway experiments on consumer Li-ion batteries with metal-oxide and olivin-type cathodes. *RSC Advances* 4, 3633–3642. doi:10.1039/c3ra45748f.
- Golubkov, A.W., Scheikl, S., Planteu, R., Voitic, G., Wiltsche, H., Stangl, C., Fauler, G., Thaler, A., Hacker, V., 2015. Thermal runaway of commercial 18650 Li-ion batteries with LFP and NCA cathodes - impact of state of charge and overcharge. *RSC Adv.* 5, 57171–57186. doi:10.1039/C5RA05897J.
- Hatchard, T.D., MacNeil, D.D., Basu, A., Dahn, J.R., 2001. Thermal Model of Cylindrical and Prismatic Lithium-Ion Cells. *Journal of The Electrochemical Society* 148, A755–A761. doi:10.1149/1.1377592.
- Hatchard, T.D., Macneil, D.D., Stevens, D.A., Christensen, L., Dahn, J.R., 2000. Importance of Heat Transfer by Radiation in Li-Ion Batteries during Thermal Abuse. *Electrochemical and Solid-State Letters* 3, 305–308.
- International Energy Agency, 2016. Global EV Outlook 2016: Beyond one million electric cars. URL: https://www.iea.org/publications/freepublications/publication/Global_EV_Outlook_2016.pdf. (accessed August 2016).
- IRENA, IEA-ETSAP, 2012. Technology Brief - Electricity Storage. URL: <https://www.irena.org/DocumentDownloads/Publications/IRENA-ETSAP%20Tech%20Brief%20E18%20Electricity-Storage.pdf>. (accessed September 2016).
- Ishikawa, H., Mendoza, O., Sone, Y., Umeda, M., 2012. Study of thermal deterioration of lithium-ion secondary cell using an accelerated rate calorimeter (ARC) and AC impedance method. *Journal of Power Sources* 198, 236–242. doi:10.1016/j.jpowsour.2011.09.067.
- Jhu, C.Y., Wang, Y.W., Wen, C.Y., Chiang, C.C., Shu, C.M., 2011. Self-reactive rating of thermal runaway hazards on 18650 lithium-ion batteries. *Journal of Thermal Analysis and Calorimetry* 106, 159–163. doi:10.1007/s10973-011-1452-6.
- Jhu, C.Y., Wang, Y.W., Wen, C.Y., Shu, C.M., 2012. Thermal runaway potential of LiCoO_2 and $\text{Li}(\text{Ni}_{1/3}\text{Co}_{1/3}\text{Mn}_{1/3})\text{O}_2$ batteries determined with adiabatic calorimetry methodology. *Applied Energy* 100, 127–131. doi:10.1016/j.apenergy.2012.05.064.
- Jiang, J., Dahn, J.R., 2004a. ARC studies of the reaction between LiFePO_4 and LiPF_6 or LiBOB EC/DEC electrolytes. *Electrochemistry Commu-*

- nications 6, 724–728. doi:[10.1016/j.elecom.2004.05.004](https://doi.org/10.1016/j.elecom.2004.05.004).
- Jiang, J., Dahn, J.R., 2004b. ARC studies of the thermal stability of three different cathode materials: LiCoO₂; Li[Ni_{0.1}Co_{0.8}Mn_{0.1}]O₂; and LiFePO₄, in LiPF₆ and LiBoB EC/DEC electrolytes. *Electrochemistry Communications* 6, 39–43. doi:[10.1016/j.elecom.2003.10.011](https://doi.org/10.1016/j.elecom.2003.10.011).
- Jiang, J., Fortier, H., Reimers, J.N., Dahn, J.R., 2004. Thermal Stability of 18650 Size Li-Ion Cells Containing LiBOB Electrolyte Salt. *Journal of The Electrochemical Society* 151, A609–A613. doi:[10.1149/1.1667520](https://doi.org/10.1149/1.1667520).
- Khakani, S.E., Rochefort, D., MacNeil, D.D., 2016. Arc study of lifepo4 with different morphologies prepared via three synthetic routes. *Journal of The Electrochemical Society* 163, A1311–A1316. doi:[10.1149/2.0801607jes](https://doi.org/10.1149/2.0801607jes), [arXiv:http://jes.ecsdl.org/content/163/7/A1311.full.pdf+html](http://jes.ecsdl.org/content/163/7/A1311.full.pdf+html).
- Kim, T.H., Park, J.S., Chang, S.K., Choi, S., Ryu, J.H., Song, H.K., 2012. The Current Move of Lithium Ion Batteries Towards the Next Phase. *Advanced Energy Materials* 2, 860–872. doi:[10.1002/aenm.201200028](https://doi.org/10.1002/aenm.201200028).
- Kvasha, A., Gutiérrez, C., Osa, U., de Meatza, I., Blazquez, J.A., Macicior, H., Urdampilleta, I., 2018. A comparative study of thermal runaway of commercial lithium ion cells. *Energy* 159, 547–557. doi:<https://doi.org/10.1016/j.energy.2018.06.173>.
- Larsson, F., Mellander, B.E., 2014. Abuse by External Heating , Overcharge and Short Circuiting of Commercial Lithium-Ion Battery Cells. *Journal of The Electrochemical Society* 161, A1611–A1617. doi:[10.1149/2.0311410jes](https://doi.org/10.1149/2.0311410jes).
- Leadbetter, J., Swan, L.G., 2012. Selection of battery technology to support grid-integrated renewable electricity. *Journal of Power Sources* 216, 376–386. doi:[10.1016/j.jpowsour.2012.05.081](https://doi.org/10.1016/j.jpowsour.2012.05.081).
- Lei, B., Zhao, W., Ziebert, C., Uhlmann, N., Rohde, M., Seifert, H., 2017. Experimental Analysis of Thermal Runaway in 18650 Cylindrical Li-Ion Cells Using an Accelerating Rate Calorimeter. *Batteries* 3, 14. doi:[10.3390/batteries3020014](https://doi.org/10.3390/batteries3020014).
- Li, Z., Huang, J., Yann, B., Metzler, V., Zhang, J., 2014. A review of lithium deposition in lithium-ion and lithium metal secondary batteries. *Journal of Power Sources* 254, 168–182. doi:[10.1016/j.jpowsour.2013.12.099](https://doi.org/10.1016/j.jpowsour.2013.12.099).
- Lisbona, D., Snee, T., 2011. A review of hazards associated with primary lithium and lithium-ion batteries. *Process Safety and Environmental Protection* 89, 434–442. doi:[10.1016/j.psep.2011.06.022](https://doi.org/10.1016/j.psep.2011.06.022).
- Liu, X., Wu, Z., Stolarov, S.I., Denlinger, M., Masias, A., Snyder, K., 2016. Heat release during thermally-induced failure of a lithium ion battery: Impact of cathode composition. *Fire Safety Journal* 85, 10–22. doi:[10.1016/j.firesaf.2016.08.001](https://doi.org/10.1016/j.firesaf.2016.08.001).
- Lopez, C.F., Jeevarajan, J.A., Mukherjee, P.P., 2015. Characterization of Lithium-Ion Battery Thermal Abuse Behavior Using Experimental and Computational Analysis. *Journal of The Electrochemical Society* 162, A2163–A2173. doi:[10.1149/2.0751510jes](https://doi.org/10.1149/2.0751510jes).
- Lu, T.Y., Chiang, C.C., Wu, S.H., Chen, K.C., Lin, S.J., Wen, C.Y., Shu, C.M., 2013. Thermal hazard evaluations of 18650 lithium-ion batteries by an adiabatic calorimeter. *Journal of Thermal Analysis and Calorimetry* 114, 1083–1088. doi:[10.1007/s10973-013-3137-9](https://doi.org/10.1007/s10973-013-3137-9).
- MacNeil, D.D., Christensen, L., Landucci, J., Paulsen, J.M., Dahn, J.R., 2000. An Autocatalytic Mechanism for the Reaction of Li_xCoO₂ in Electrolyte at Elevated Temperature. *Journal of The Electrochemical Society* 147, 970–979. doi:[10.1149/1.1393299](https://doi.org/10.1149/1.1393299).
- MacNeil, D.D., Lu, Z., Chen, Z., Dahn, J.R., 2002. A comparison of the electrode/electrolyte reaction at elevated temperatures for various Li-ion battery cathodes. *Journal of Power Sources* 108, 8–14.
- Melcher, A., Ziebert, C., Rohde, M., Seifert, H.J., 2016. Modeling and simulation of the thermal runaway behavior of cylindrical Li-ion cells-computing of critical parameters. *Energies* 9, 1–19. doi:[10.3390/en9040292](https://doi.org/10.3390/en9040292).
- Mendoza-Hernandez, O.S., Ishikawa, H., Nishikawa, Y., Maruyama, Y., Umeda, M., 2015. Cathode material comparison of thermal runaway behavior of Li-ion cells at different state of charges including over charge. *Journal of Power Sources* 280, 499–504. doi:[10.1016/j.jpowsour.2015.01.143](https://doi.org/10.1016/j.jpowsour.2015.01.143).
- Ohsaki, T., Kishi, T., Kuboki, T., Takami, N., Shimura, N., Sato, Y., Sekino, M., Satoh, A., 2005. Overcharge reaction of lithium-ion batteries.

- Journal of Power Sources 146, 97–100. doi:[10.1016/j.jpowsour.2005.03.105](https://doi.org/10.1016/j.jpowsour.2005.03.105).
- Palizban, O., Kauhaniemi, K., 2016. Energy storage systems in modern grids - Matrix of technologies and applications. *Journal of Energy Storage* 6, 248–259. doi:[10.1016/j.est.2016.02.001](https://doi.org/10.1016/j.est.2016.02.001).
- Parhizi, M., Ahmed, M.B., Jain, A., 2017. Determination of the core temperature of a Li-ion cell during thermal runaway. *Journal of Power Sources* 370, 27–35. doi:[10.1016/j.jpowsour.2017.09.086](https://doi.org/10.1016/j.jpowsour.2017.09.086).
- Peng, P., Jiang, F., 2016. Thermal safety of lithium-ion batteries with various cathode materials: A numerical study. *International Journal of Heat and Mass Transfer* 103, 1008–1016. doi:[10.1016/j.ijheatmasstransfer.2016.07.088](https://doi.org/10.1016/j.ijheatmasstransfer.2016.07.088).
- Perea, A., Paoletta, A., Dubé, J., Champagne, D., Mauger, A., Zaghbi, K., 2018. State of charge influence on thermal reactions and abuse tests in commercial lithium-ion cells. *Journal of Power Sources* 399, 392 – 397. doi:<https://doi.org/10.1016/j.jpowsour.2018.07.112>.
- Placke, T., Kloepsch, R., Dühnen, S., Winter, M., 2017. Lithium ion, lithium metal, and alternative rechargeable battery technologies: the odyssey for high energy density. *Journal of Solid State Electrochemistry* 21, 1939–1964. doi:[10.1007/s10008-017-3610-7](https://doi.org/10.1007/s10008-017-3610-7).
- Richard, M.N., Dahn, J.R., 1999a. Accelerating Rate Calorimetry Study on the Thermal Stability of Lithium Intercalated Graphite in Electrolyte I. Experimental. *Journal of The Electrochemical Society* 146, 2068–2077. doi:[10.1149/1.1391894](https://doi.org/10.1149/1.1391894).
- Richard, M.N., Dahn, J.R., 1999b. Accelerating Rate Calorimetry Study on the Thermal Stability of Lithium Intercalated Graphite in Electrolyte. II. Modeling the Results and Predicting Differential Scanning Calorimeter Curves. *Journal of The Electrochemical Society* 146, 2078–2084. doi:[10.1149/1.1391894](https://doi.org/10.1149/1.1391894).
- Roth, E.P., Doughty, D.H., 2004. Thermal abuse performance of high-power 18650 Li-ion cells. *Journal of Power Sources* 128, 308–318. doi:[10.1016/j.jpowsour.2003.09.068](https://doi.org/10.1016/j.jpowsour.2003.09.068).
- Spotnitz, R., Franklin, J., 2003. Abuse behavior of high-power, lithium- ion cells. *Journal of Power Sources* 113, 81–100.
- Takahashi, M., Tobishima, S.i., Takei, K., Sakurai, Y., 2002. Reaction behavior of LiFePO₄ as a cathode material for rechargeable lithium batteries. *Solid State Ionics* 148, 283–289.
- Tobishima, S.i., Yamaki, J.i., 1999. A consideration of lithium cell safety. *Journal of Power Sources* 81-82, 882–886. doi:[10.1016/S0378-7753\(98\)00240-7](https://doi.org/10.1016/S0378-7753(98)00240-7).
- Verma, P., Maire, P., Novák, P., 2010. A review of the features and analyses of the solid electrolyte interphase in Li-ion batteries. *Electrochimica Acta* 55, 6332–6341. doi:[10.1016/j.electacta.2010.05.072](https://doi.org/10.1016/j.electacta.2010.05.072), [arXiv:arXiv:1011.1669v3](https://arxiv.org/abs/1011.1669v3).
- Waldmann, T., Hogg, B.I., Wohlfahrt-Mehrens, M., 2018. Li plating as unwanted side reaction in commercial li-ion cells – a review. *Journal of Power Sources* 384, 107 – 124. doi:<https://doi.org/10.1016/j.jpowsour.2018.02.063>.
- Wang, Q., Ping, P., Zhao, X., Chu, G., Sun, J., Chen, C., 2012. Thermal runaway caused fire and explosion of lithium ion battery. *Journal of Power Sources* 208, 210–224. doi:[10.1016/j.jpowsour.2012.02.038](https://doi.org/10.1016/j.jpowsour.2012.02.038).
- Wen, C.Y., Jhu, C.Y., Wang, Y.W., Chiang, C.C., Shu, C.M., 2012. Thermal runaway features of 18650 lithium-ion batteries for LiFePO₄ cathode material by DSC and VSP2. *Journal of Thermal Analysis and Calorimetry* 109, 1297–1302. doi:[10.1007/s10973-012-2573-2](https://doi.org/10.1007/s10973-012-2573-2).
- Yamada, A., Chung, S.C., Hinokuma, K., 2001. Optimized LiFePO₄ for Lithium Battery Cathodes. *Journal of Electroanalytical Society* 148, 224–229. doi:[10.1149/1.1348257](https://doi.org/10.1149/1.1348257).
- Zhang, S.S., 2014. Insight into the Gassing Problem of Li-ion Battery. *Frontiers in Energy Research* 2, 1–4. doi:[10.3389/fenrg.2014.00059](https://doi.org/10.3389/fenrg.2014.00059).